



Fermi National Accelerator Laboratory

FERMILAB-Conf-97/408-E

CDF

From HERA to the Tevatron: A Scaling Law in Hard Diffraction

K. Goulios

For the CDF Collaboration

*Fermi National Accelerator Laboratory
P.O. Box 500, Batavia, Illinois 60510*

December 1997

Published Proceedings of the *27th International Symposium on Multiparticle Dynamics (ISMD 97)*,
Frascati, Italy, September 8-12, 1997

Disclaimer

This report was prepared as an account of work sponsored by an agency of the United States Government. Neither the United States Government nor any agency thereof, nor any of their employees, makes any warranty, expressed or implied, or assumes any legal liability or responsibility for the accuracy, completeness, or usefulness of any information, apparatus, product, or process disclosed, or represents that its use would not infringe privately owned rights. Reference herein to any specific commercial product, process, or service by trade name, trademark, manufacturer, or otherwise, does not necessarily constitute or imply its endorsement, recommendation, or favoring by the United States Government or any agency thereof. The views and opinions of authors expressed herein do not necessarily state or reflect those of the United States Government or any agency thereof.

Distribution

Approved for public release; further dissemination unlimited.

December 4, 1997

1

From HERA to the Tevatron: a scaling law in hard diffraction

K. Goulianos^{a*}^a(The CDF Collaboration)

Rockefeller University, 1230 York Avenue, New York, NY 10021, USA (dino@physics.rockefeller.edu)

Results on hard diffraction from CDF are reviewed and compared with predictions based on the diffractive structure function of the proton measured in deep inelastic scattering at HERA. The predictions are generally larger than the measured rates by a factor of ~ 6 , suggesting a breakdown of conventional factorization. Correct predictions are obtained by scaling the rapidity gap probability distribution of the diffractive structure function to the total integrated gap probability. The scaling of the gap probability is traced back to the pomeron flux renormalization hypothesis, which was introduced to unitarize the soft diffraction amplitude.

1. INTRODUCTION

The term “hard diffraction” refers to a class of hadronic diffractive processes that incorporate a hard scattering. In this paper, we summarize the CDF results on hard diffraction [1–6] and compare them with predictions based on the diffractive structure function (SF) of the proton measured in $e^+p \rightarrow e^+ + [\gamma^*p \rightarrow Xp]$ deep inelastic scattering (DIS) at HERA [7,8]. Our comparison between CDF and HERA results has been reported in two previous papers[5,6], parts of which are reproduced here.

Hadronic diffraction is believed to be mediated by the exchange of the pomeron, which carries the quantum numbers of the vacuum. In the framework of QCD, pomeron exchange must involve the exchange of $q\bar{q}$ and/or gg pairs in a color-singlet state. However, the question arises whether the pomeron, although virtual, has a *unique* partonic structure, as do real hadrons. Such a structure, if it exists, could be probed in hard diffractive processes. Figure 1 shows the event topology for dijet production in single diffraction (SD), double diffraction (DD), and double pomeron exchange (DPE). Since there is no color exchanged between the colorless pomeron and the parent nucleon, a rapidity gap (region devoid of particles) emerges as a characteristic signature of pomeron

exchange, as shown schematically in the $\eta - \phi$ plots of Fig. 1. Such gaps can be used to tag diffractive production. Another way of tagging diffraction is provided by the recoil \bar{p} or p in SD or in DPE. The CDF Collaboration has reported results for hard diffraction in $\bar{p}p$ collisions at $\sqrt{s} = 1800$ GeV using both tagging techniques.

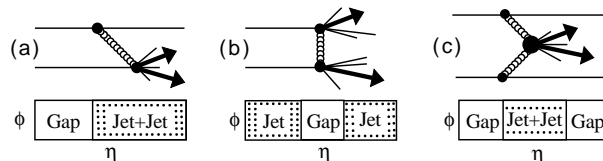


Figure 1. Dijet production diagrams and event topologies for (a) single diffraction (b) double diffraction and (c) double pomeron exchange.

At HERA, where ~ 28 GeV electrons are brought into collision with ~ 800 GeV protons ($\sqrt{s} \approx 300$ GeV), diffraction has been studied both in photoproduction and in high Q^2 DIS. The H1 and ZEUS Collaborations have measured the diffractive structure function of the proton and its internal factorization properties. Figure 2 shows the kinematics of a DIS diffractive collision.

In analogy with the $F_2(Q^2, x)$ structure function, the 4-variable diffractive structure function (DSF) of the proton, $F_2^{D(4)}(Q^2, x, \xi, t)$, is defined through the cross section equation

$$\frac{d^4\sigma}{dQ^2 dx d\xi dt} = \frac{4\pi\alpha^2}{x Q^4} \cdot f(y) \cdot F_2^{D(4)}(Q^2, x, \xi, t) \quad (1)$$

*Presented at the XXVII International Symposium on Multiparticle Dynamics, Laboratori Nazionali di Frascati-INFN, 8-12 September 1997.

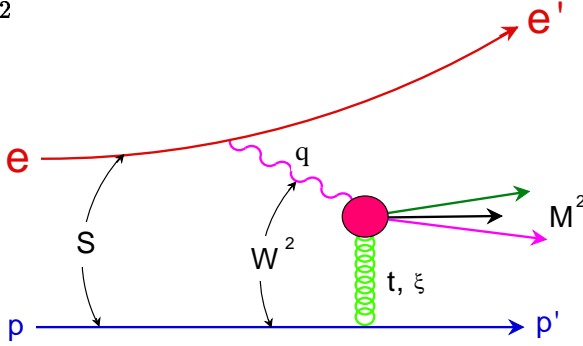


Figure 2. Schematic diagram of a diffractive DIS collision involving a virtual photon, emitted by an electron, and a virtual pomeron, emitted by a proton.

where x and y are the Bjorken DIS variables, $f(y) \equiv 2 - 2y + y^2/[2(1+R)]$, and ξ is the fraction of the proton's momentum taken by the pomeron. The t -integrated DSF, $F_2^{D(3)}$, was determined from the data by assuming $R = 0$ in $f(y)$. The reported measured values for $F_2^{D(3)}$ correspond to cross sections given by

$$\frac{d^3\sigma}{dQ^2 d\beta d\xi} \Big|_{|t| \leq 1} \equiv \frac{4\pi\alpha^2}{\beta Q^4} \cdot f(y) \cdot F_2^{D(3)}(Q^2, \beta, \xi) \quad (2)$$

where $\beta \equiv x/\xi$ represents the fraction of the momentum of the pomeron carried by the interacting quark. In section 3 we will use the measured $F_2^{D(3)}$ structure function to predict the rate for diffractive W production at the Tevatron and compare the prediction with the value measured by CDF.

2. HARD DIFFRACTION IN CDF

2.1. Results using rapidity gaps

Four processes were studied by CDF using the rapidity gap method to tag diffraction:

- Diffractive dijet production
- Diffractive W production
- Dijet production by color-singlet exchange
- Diffractive heavy flavor production

The components of the CDF detector relevant to these studies are [9] the Beam-Beam Counters (BBC), the Central Tracking Chamber (CTC)

and the calorimeters. The BBC consist of a square array of 16 scintillation counters placed at $\pm z$ position of 6 m from the center of the detector. The calorimeters have a tower geometry with segmentation of 0.1 units in η and 15° (5° for $|\eta| > 1.1$) in ϕ . The η -coverage is:

BBC	$3.2 < \eta < 5.9$
CTC	$ \eta < 1.8$
CAL: central	$ \eta < 1.1$
CAL: plug	$1.1 < \eta < 2.4$
CAL: forward	$2.2 < \eta < 4.2$

A “particle” is defined as a hit in a BBC, a track with $P_T > 300$ MeV in the CTC, or a calorimeter tower with measured $E_T > 200$ MeV (corrected $E_T > \sim 300$ MeV), except for the region $2.4 < |\eta| < 4.2$ for which the requirement is a tower energy of $E > 1.5$ GeV.

2.2. Diffractive dijet production

CDF searched for diffractive dijet production in a sample of 30352 dijet events with a single-vertex (to exclude events from multiple interactions), in which the two leading jets have $E_T > 20$ GeV and are both at $\eta < 1.8$ or $\eta > 1.8$. No requirement was imposed on the presence or kinematics of extra jets in an event. Figure 3 shows the correlation of the BBC and forward ($|\eta| > 2.4$) calorimeter tower multiplicities in the η -region opposite the dijet system. The excess in the 0-0 bin is attributed to diffractive production. After subtracting the non-diffractive background and correcting for the single-vertex selection cut, for detector live-time acceptance and for the rapidity gap acceptance (0.70 ± 0.03), calculated using the POMPYT Monte Carlo program [1] with pomeron $\xi < 0.1$, the “Gap-Jet-Jet” fraction (ratio of diffractive to non-diffractive dijet events) was found to be

$$R_{GJJ} = [0.75 \pm 0.05(\text{stat}) \pm 0.09(\text{syst})]\% = (0.75 \pm 0.10)\% \\ (E_T^{jet} > 20 \text{ GeV}, |\eta|^{jet} > 1.8, \eta_1 \eta_2 > 0, \xi < 0.1)$$

Figure 4 shows pomeron- ξ distributions of dijet events generated by a POMPYT Monte Carlo simulation for $\xi < 0.1$ and a hard gluon pomeron structure. The jets were required to have $E_T^{jet} > 20$ GeV and be in the region $1.8 < |\eta| < 3.5$ with $\eta_1 \cdot \eta_2 > 0$.

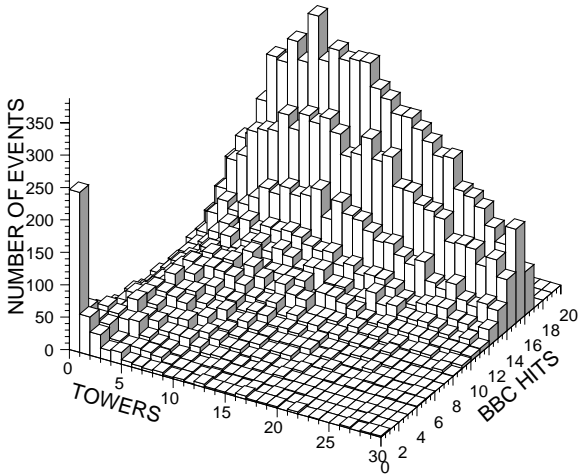


Figure 3. Tower versus BBC multiplicity for dijet events with both jets at $\eta > 1.8$ or $\eta < 1.8$.

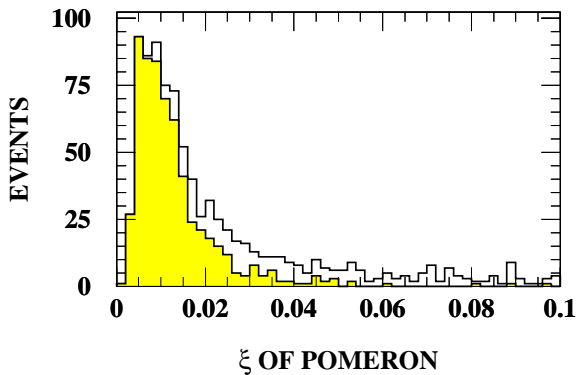


Figure 4. Monte Carlo pomeron ξ distributions for diffractive dijet events with jet $E_T > 20$ GeV and $1.8 < |\eta| < 3.5$ generated by POMPYYT using a hard-gluon pomeron structure. The shaded area represents the subset of Monte Carlo events with zero BBC and forward calorimeter multiplicities, corresponding to the data in the (0,0) bin of Fig. 3.

2.3. Diffractive W production

CDF made the first observation [2] of diffractive W s and measured the W production rate using a sample of 8246 events with an isolated central e^+ or e^- ($|\eta| < 1.1$) of $E_T > 20$ GeV and missing transverse energy $\cancel{E}_T > 20$ GeV. In searching for diffractive events, CDF studied the correlations of the BBC multiplicity, N_{BBC} , with the sign of the electron- η , η_e , or the sign of its charge, C_e . In a diffractive $W^\pm \rightarrow e^\pm \nu$ event produced in a \bar{p} collision with a pomeron emitted by the proton, a rapidity gap is expected at positive η (p -direction), while the lepton is boosted towards negative η (angle-gap correlation). Also, since the pomeron is quark-flavor symmetric, and since, from energy considerations, mainly valence quarks from the \bar{p} participate in producing the W , approximately twice as many electrons as positrons are expected (charge-gap correlation).

Figure 5 shows the BBC versus tower multiplicity for two event samples characterized by the correlation between the pseudorapidity of the BBC whose multiplicity is plotted, η_{BBC} , and the η_e or C_e , as follows: (a) *doubly-correlated* events, for which $\eta_e \cdot C_e > 0$ and $\eta_e \cdot \eta_{BBC} < 0$, and (b) *doubly-anticorrelated* events, for which $\eta_e \cdot C_e > 0$ and $\eta_e \cdot \eta_{BBC} > 0$. Monte Carlo simulations show that diffractive W events are expected to have low BBC or tower multiplicities (in the range 0-3), and that there should be ~ 4 times as many doubly-correlated than doubly-anticorrelated events. This diffractive signature is satisfied by the small number of events at low multiplicities in Fig. 5. Figure 6 shows BBC multiplicities and asymmetries between multiplicities for various event samples, as explained in the figure, for events with tower multiplicity less than eight. An excess of events is observed in the zero bin of all correlated event samples over the number in the corresponding anticorrelated samples. The probability that the observed excess is caused by fluctuations in the non-diffractive background was estimated to be 1.1×10^{-4} .

Correcting for acceptance, the ratio of diffractive to non-diffractive W production is:
 $R_W = [1.15 \pm 0.51(stat) \pm 0.20(syst)]\%$ ($\xi < 0.1$)
 Figure 7 shows pomeron- ξ distributions of W events generated by POMPYYT.

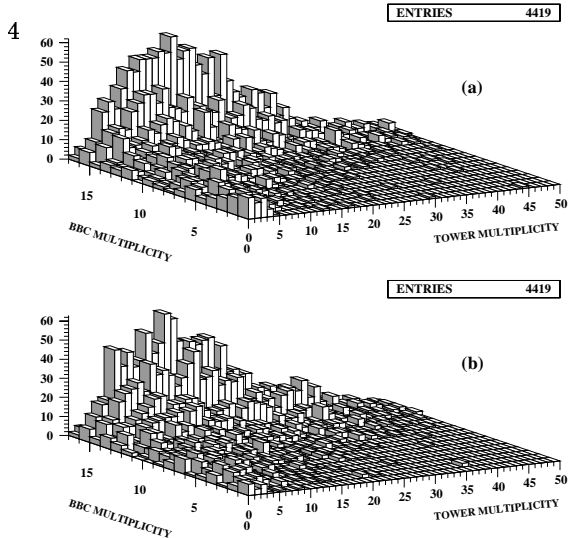


Figure 5. Tower versus BBC multiplicity for W events: (a) (angle \otimes charge)-correlated; (b) (angle \otimes charge)-anticorrelated.

2.4. The gluon fraction of the pomeron

By combining the diffractive W and dijet results, CDF extracted the gluon fraction of the pomeron, f_g . Assuming the standard pomeron flux, the measured W and dijet fractions trace curves in the plane of D versus f_g , where D is the total momentum fraction carried by the quarks and gluons in the pomeron. Figure 8 shows the $\pm 1\sigma$ curves corresponding to the results. From the diamond-shaped overlap of the W and dijet curves, CDF obtained $f_g = 0.7 \pm 0.2$. This result, which is independent of the pomeron flux normalization, agrees with the result obtained by ZEUS [7] from DIS and dijet photoproduction (dashed-dotted line in Fig. 8). For the D -fraction, CDF obtained the value $D = 0.18 \pm 0.04$. In the next section we will show that the decrease of the D -fraction from HERA to the Tevatron can be accounted for by the pomeron flux renormalization factor. The dashed lines are the $\pm 1\sigma$ curves of the UA8 diffractive dijet results [10]. To compare UA8 with CDF, the UA8 fractions must first be multiplied by the ratio of the renormalization factors at the two energies, which is [11] $D_{CDF}/D_{UA8} \approx 0.7$. Within the errors, the results of the two experiments are in good agreement.

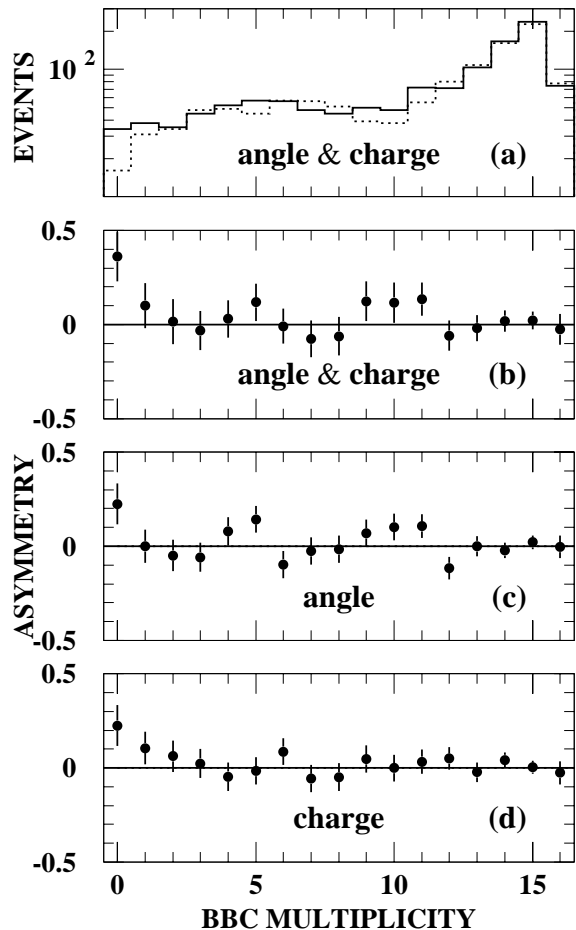


Figure 6. BBC multiplicities, N_{BBC} , for events with $\eta_e \cdot \eta_{BBC} < 0$ (angle-correlated), $C_e \cdot \eta_{BBC} < 0$ (charge-correlated), $\eta_e \cdot \eta_{BBC} > 0$ (angle-anticorrelated), and $C_e \cdot \eta_{BBC} > 0$ (charge-anticorrelated): (a) The *doubly-correlated* (*anti-correlated*, dotted) distributions for events with $\eta_e \cdot C_e > 0$ and $\eta_e \cdot \eta_{BBC} < 0$ ($\eta_e \cdot \eta_{BBC} > 0$); (b) bin-by-bin asymmetry (difference divided by sum) of the above two distributions. The excess seen in the first bin is the signature expected from diffractive events with a rapidity gap. An excess is also seen in the individual angle (c) and charge (d) asymmetries, as expected. The probability that the observed excess is caused by fluctuations in the non-diffractive background is estimated to be 1.1×10^{-4} .

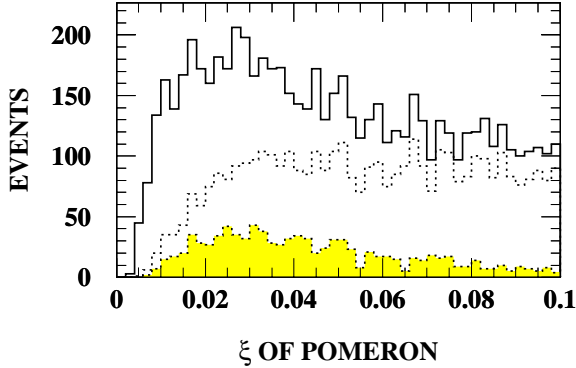


Figure 7. Monte Carlo pomeron ξ distributions for diffractive W events generated by POMPYT using a hard-quark pomeron structure: (*solid line*) all events; (*dotted line*) events with a central electron; (*shaded area*) events with a central electron and 0, 1 or 2 hits in the (angle \oplus charge)-correlated BBC (corresponding to the signal).

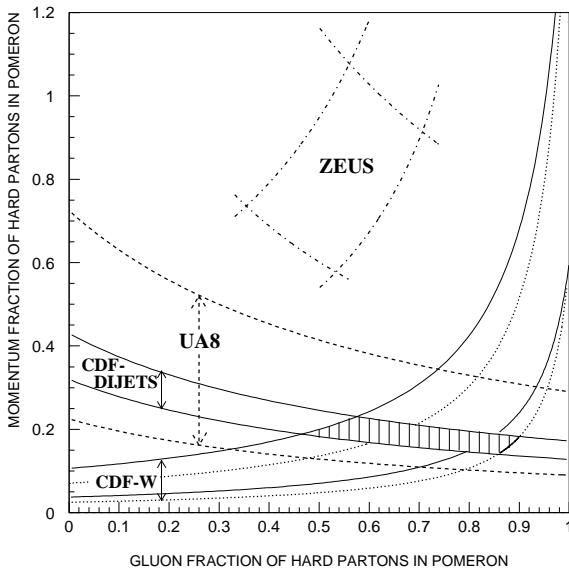


Figure 8. Sum of momentum fraction of partons in the pomeron versus gluon fraction.

2.5. Dijet production by color-singlet exchange

Results on dijet events produced by color-singlet exchange have been published by CDF [12] and $D\bar{O}$ [13] (Tevatron) and by ZEUS [14] (HERA). Recently, a new measurement of the rate of such events and its dependence on jet E_T and rapidity interval between the jets has been reported by CDF [3,4]. In a sample of 10200 single-vertex events with two jets of transverse energy $E_T^{jet} > 20$ GeV, pseudorapidity $1.8 < |\eta| < 3.5$ and $\eta_1 \cdot \eta_2 < 0$, a search was made for events with a rapidity gap in the region of $|\eta| < 1.0$ between the jets. The background of normal color octet exchange events that happen to have a rapidity gap in this region due to multiplicity fluctuations was evaluated by using as a template the track (tower) multiplicity distribution of a sample of dijet events with the two jets in the same hemisphere (the same sample that was used in the diffractive dijet analysis). The multiplicity of the same-side (SS) dijet events was evaluated within $|\eta| < 1.2$ to ensure the same mean multiplicity as that of the opposite-side (OS) event sample. Figure 9 shows the track and tower multiplicity distributions for OS and (normalized) SS dijet events and their asymmetries, defined as the bin-by-bin difference over sum of the corresponding multiplicities. The ratio of “Jet-Gap-Jet” to all events was evaluated from the excess OS over SS events in the low multiplicity bins (0 for tracks and 0-2 for towers), after correcting for the single-vertex cut acceptance:

$$R_{JJ} = 1.13 \pm 0.12(stat) \pm 0.11(syst)\% = (1.13 \pm 0.16)\%$$

$$(E_T^{jet} > 20 \text{ GeV}, |\eta^{jet}| > 1.8, \eta_1\eta_2 < 0)$$

This value of R is consistent with the published CDF and $D\bar{O}$ results.

In addition to measuring the overall ratio R , CDF studied the properties of a sample of 221 “gap” events with zero tracks and 0,1 or 2 towers within $|\eta| < 1$. This sample contains an estimated 15% normal color-octet exchange events, in which the gap is due to multiplicity fluctuations. For this reason, the properties of the gap events were compared with those of a “control” sample consisting of events with 1, 2 or 3 tracks and up to 6 towers. Figure 10 shows normalized ratios of gap

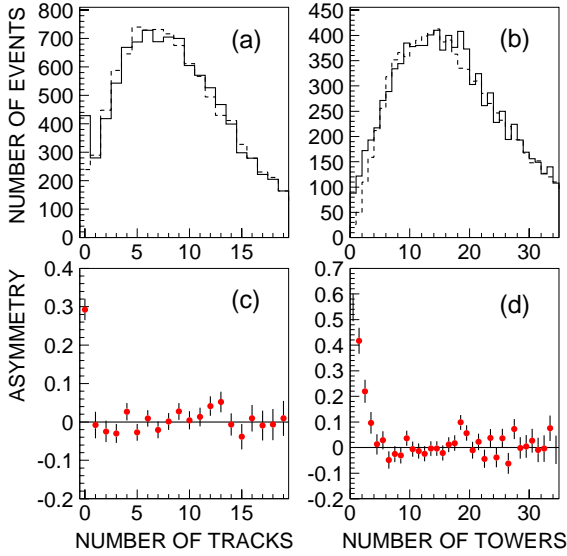


Figure 9. (*top*) Multiplicity distributions for OS (solid, $|\eta| < 1.0$) and SS (dashed, $|\eta| < 1.2$) dijet events; (*bottom*) the asymmetry (bin-by-bin difference over sum) of the distributions shown on top. The low multiplicity excess is attributed to colorless exchange.

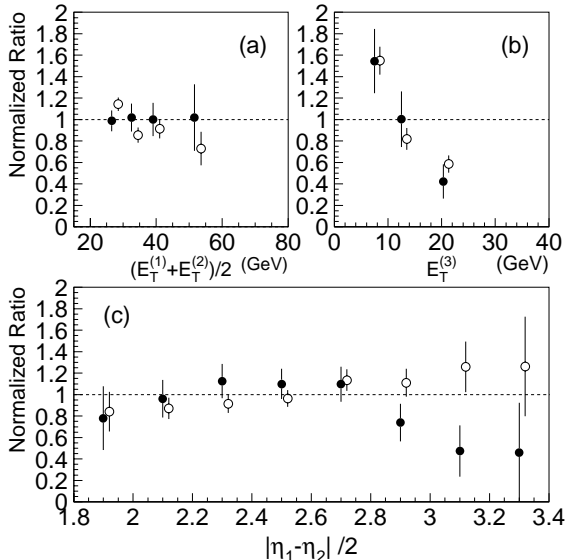


Figure 10. Normalized (to be unity on average) ratios of gap (solid points) and control sample events (open circles) over all events versus: (a) the average E_T of the two leading jets, (b) the E_T of the third jet, and (c) half the η separation between the two leading jets.

and control sample events to all events as a function of the average E_T of the two leading jets, the E_T of the third jet, and the η -separation of the two leading jets. The gap and control samples behave similarly. The colorless exchange fraction is fairly independent of jet E_T and $\Delta\eta$, decreasing somewhat at large $\Delta\eta$.

2.5.1. Diffractive heavy flavor production

Using the rapidity gap technique, a diffractive signal was observed in an inclusive electron sample of events with $7 < E_T^e < 20$ GeV and $|\eta^e| < 1.1$. A preliminary measurement of the ratio of diffractive to non-diffractive events yields

$$R \left(\frac{\text{diff}}{\text{non-diff}} \right) = [0.18 \pm 0.03 (\text{stat})]\%$$

2.6. Results using roman pots

About 1.8×10^6 events, recorded by triggering the CDF detector inclusively on a *leading* antiproton detected in a roman pot spectrometer, have been analyzed. Several more million events were collected and are currently being analyzed. The results presented here are for the kinematic region $0.05 < \xi < 0.1$ and $|t| < 2$ GeV², within which the spectrometer acceptance varies from 100% at $|t| = 0$ to $\sim 30\%$ at $|t| = 2$ GeV². Figure 11 shows the roman pot arrangement.

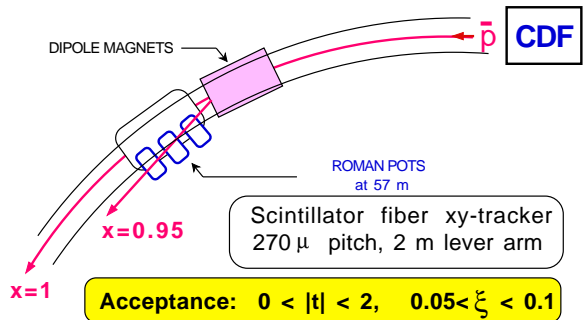


Figure 11. Schematic view of the CDF leading antiproton spectrometer

The normalization is obtained from the known inclusive single diffraction cross section measured by CDF [15]. To avoid systematic detector-related effects, each result is presented as a ratio of diffractive to non-diffractive production.

The measured ratios are compared with the corresponding predicted ratios from simulations using POMPYT for diffractive and PYTHIA for non-diffractive production.

The roman pot data were recorded during collider run 1C (winter 1995-1996). During this run, in addition to the roman pot spectrometer, two small electromagnetic “Microplug” calorimeters covering the region $4.5 < |\eta| < 5.5$ were installed in CDF to help identify and trigger on forward rapidity gaps (see Figs. 13 and 14).

2.6.1. Dijet production (\bar{p} -Jet-Jet)

The inclusive \bar{p} -triggered data contain 2503 single-vertex events with two jets of $E_T^{jet} > 10$ GeV. After corrections for non-diffractive contamination (8%) and single-vertex selection cut efficiency ($72 \pm 5\%$), the ratio of diffractive to non-diffractive events is

$$R_{\bar{p}JJ} = [0.109 \pm 0.003(stat) \pm 0.016(syst)]\% \\ (E_T^{jet} > 10 \text{ GeV}, 0.05 < \xi < 0.1, |t| < 2)$$

Assuming a hard gluon and hard quark pomeron structure with $f_g = 0.7$ and $f_q = 0.3$, as suggested by the rapidity gap diffractive dijet and W production rates, the prediction using the standard (renormalized) pomeron flux is 1.35% (0.15%). The roman pot result favors the renormalized flux. Figure 12 shows the t -dependence of the (normalized) ratio of diffractive to inclusive dijet production events as a function of t . Within the range of the measurement, $0 < |t| < 2 \text{ GeV}^2$, the ratio $R_{\bar{p}JJ}$ is independent of t .

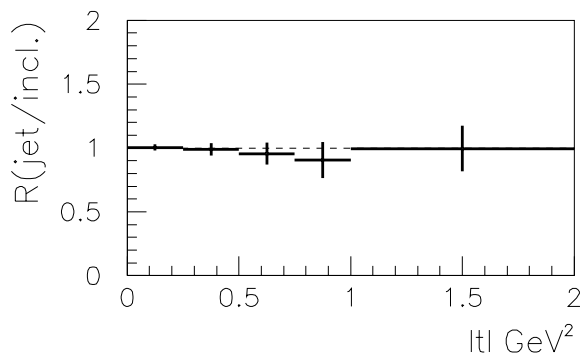


Figure 12. The (normalized) ratio of diffractive roman pot to all dijet events, $R_{\bar{p}JJ}$, versus $|t|$.

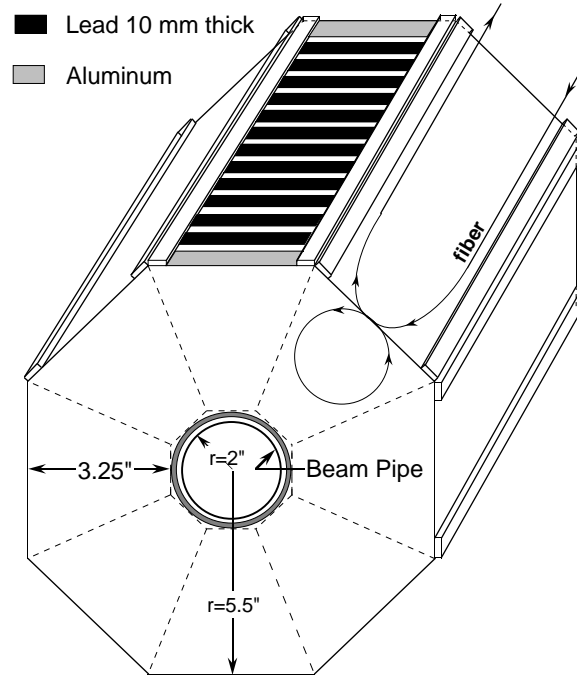


Figure 13. The “Microplug” calorimeter.

CDF in Run 1C
October 95 to February 96

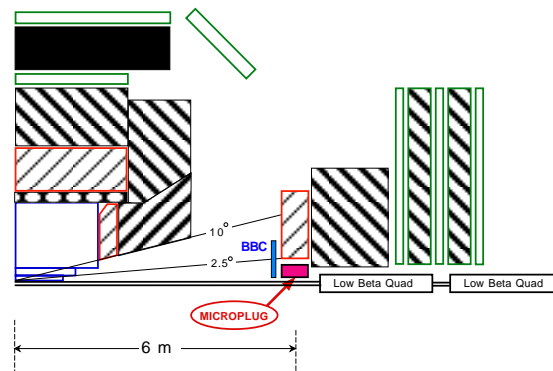


Figure 14. The CDF detector showing the Microplug position in Run 1C

2.6.2. Dijets in double-pomeron exchange (\bar{p} -Jet-Jet-Gap)

In the \bar{p} -triggered data sample, evidence was found for dijet production by double pomeron exchange in events with two jets of $E_T^{jet} > 7$ GeV and a rapidity gap in the BBC array on the proton side (Fig. 15).

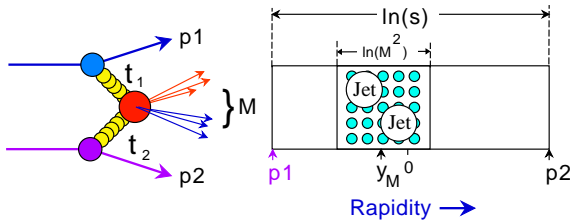


Figure 15. Kinematics of dijet production by double-pomeron exchange.

The \bar{p} trigger requires the ξ of the pomeron from the \bar{p} to be within the range $0.05 < \xi_{\bar{P}/\bar{p}} < 0.1$, while from the rapidity interval covered by the BBC and from energy considerations it is estimated that the ξ of the pomeron on the p side lies approximately within the range $0.015 < \xi_{P/p} < 0.035$. With these ξ -values, the energy in the $P-P$ center of mass system, $(\xi_{\bar{P}/\bar{p}} \cdot \xi_{P/p} \cdot s)^{\frac{1}{2}}$, is approximately in the range 50-100 GeV. In the table below, the rate of DPE dijets is compared with the rates of SD and non-diffractive (ND) dijet production. The comparison is made for jets of $E_T^{jet} > 7$ GeV.

DPE/SD	$[0.170 \pm 0.036 \pm 0.024(\text{sys})]\%$
SD/ND	$[0.160 \pm 0.002 \pm 0.024(\text{sys})]\%$
$R = \frac{(DPE/SD)}{(SD/ND)}$	1.1 ± 0.3
DPE/ND	$(2.7 \pm 0.7) \times 10^{-6}$

From factorization arguments, the ratio $R = (DPE/SD)/(SD/ND)$ is expected to be close to unity. However, as discussed above, the SD dijet rate is suppressed by a factor of ~ 10 relative to that predicted by the factorization based standard pomeron flux. Thus, the agreement of the value of R with unity indicates that approximately the same suppression factor applies to both the proton and antiproton sides in DPE. This result supports the hypothesis of pomeron flux renormalization [11].

3. From HERA to the Tevatron

The diffractive structure function $F_2^{D(3)}$ measured in DIS at HERA (see Eq. 2 in section 1) can be used directly to calculate the rate of diffractive W -boson production in $p\bar{p}$ collisions at $\sqrt{s} = 1800$ GeV. Such a calculation yields [5] $R_W = 6.7\%$ for the ratio of diffractive to non-diffractive W production (a similar result has been obtained [16] by L. Alvero, J. Collins, J. Terron and J. Whitmore). The measured value [2] $R_W = (1.15 \pm 0.55)\%$ is smaller than the predicted 6.7% by a factor of 0.17 ± 0.08 . The deviation of this factor from unity represents a *breakdown of factorization*.

Assuming that the rapidity gap probability (ξ -distribution) in $F_2^{D(3)}$ (Eq. 2) scales to the total (integrated over all available phase space) gap probability, it has been shown [5] that the ratio of the scaling factors from HERA to the Tevatron is 0.19. This ratio agrees with the discrepancy factor of 0.17 ± 0.08 between the measured R_W and the standard factorization prediction, as well as (or equivalently) with the momentum sum rule discrepancy $D = 0.18 \pm 0.04$ obtained from the comparison of the diffractive W and dijet rates (see section 2.4). Thus, the diffractive structure function with a *scaled* gap probability provides a “transatlantic diffractive bridge” connecting HERA with the Tevatron.

4. A scaling law in diffraction

The scaling of the gap probability in the diffractive structure function is equivalent to the pomeron flux renormalization scheme proposed to unitarize the soft diffraction triple-pomeron amplitude [11]. Thus, the breakdown of factorization in hard diffraction is traced back to the breakdown observed in soft diffraction [5,6,11].

In both cases, soft and hard, factorization breaks down in order to preserve unitarity. The interesting fact is that the breakdown occurs in a way that respects a scaling law, namely the scaling of the (ξ, t) -differential gap probability to the total gap probability, integrated over all available (ξ, t) -space for any given process.

In soft diffraction, there are two spectacular confirmations of this scaling law: the s -

dependence of the total single diffraction dissociation cross section, shown in Fig. 16 [11], and that of the differential cross section $d^2\sigma_{sd}/dt dM^2|_{t=0}$, shown in Fig. 17 [5,6,17] for $t = -0.05 \text{ GeV}^2$ ($t \approx 0$). In Fig. 16, it is seen that the prediction of the renormalized flux, which is the pomeron flux with its integral normalized to unity, describes well the data all the way from $\sqrt{s} = 22 \text{ GeV}$, where the flux integral becomes unity, to the CDF measurements at $\sqrt{s} = 546$ and 1800 GeV . In contrast, the standard triple-pomeron flux prediction rises within this energy range by almost an order of magnitude. In Fig. 17, the differential cross section $d^2\sigma_{sd}/dt dM^2|_{t=0.05}$ follows *over six orders of magnitude* the approximately simple exponential (s -scaling) behavior expected from the renormalized pomeron flux prediction (solid line), which deviates markedly from the non-scaling predictions of the standard Regge theory (dashed lines, solid line at $\sqrt{s} = 14$ and 20 GeV).

In hard diffraction, predictions made with the renormalized pomeron flux agree with the HERA data on diffractive DIS [11], as well as with the CDF data on diffractive dijet [1] and W [2] production (see also [5,6]).

5. Conclusion

Experiments at HERA and at $p\bar{p}$ Colliders show that the pomeron has a hard partonic structure, which consists of $\sim 70\%$ gluons and $\sim 30\%$ quarks. Predictions using the diffractive structure function of the proton measured in DIS at HERA are larger than the W and dijet rates measured at the Tevatron by a factor of ~ 6 . This breakdown of factorization can be accommodated by scaling the rapidity gap probability distribution, which appears in the diffractive structure function as a ξ -dependent factor multiplying a function of Q^2 and β , to the total gap probability. The scaling of the gap probability is equivalent to the pomeron flux renormalization hypothesis introduced [11] to account for the s -dependence of the soft $p\bar{p}$ single diffraction dissociation cross section.

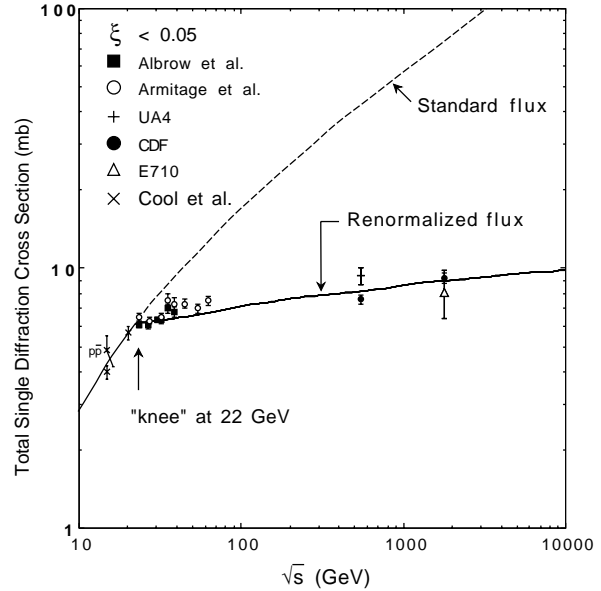


Figure 16. The $p(\bar{p}) + p \rightarrow p(\bar{p}) + X$ total single diffraction dissociation cross section as a function of center of mass energy.

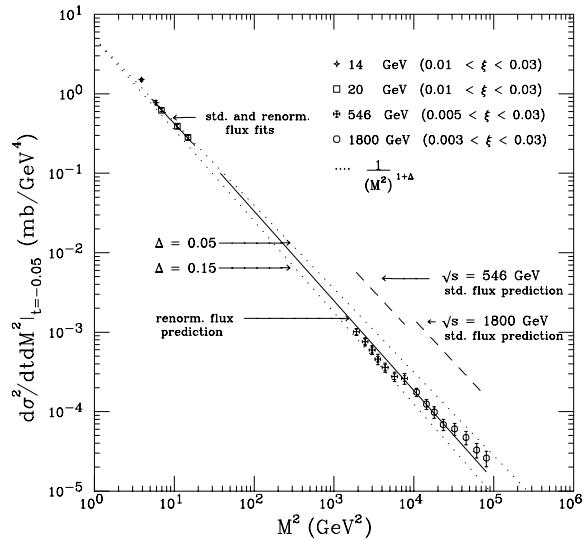


Figure 17. The $p(\bar{p}) + p \rightarrow p(\bar{p}) + X$ total single diffraction dissociation cross section $d^2\sigma_{sd}/dt dM^2|_{t=0.05}$ as a function of M^2 .

REFERENCES

1. F. Abe *et al.*, CDF Collaboration, *Measurement of diffractive dijet production at the Fermilab Tevatron*, Phys. Rev. Lett. **79** (1997) 2636.
2. F. Abe *et al.*, CDF Collaboration, *Observation of diffractive W-boson production at the Fermilab Tevatron*, Phys. Rev. Lett. **78** (1997) 2698.
3. F. Abe *et al.*, CDF Collaboration, *Dijet production by color-singlet exchange at the Fermilab Tevatron*, accepted for publication in Phys. Rev. Letters.
4. K. Goulianos, *Results on hard diffraction from CDF*, Paper to appear in Proceedings of QCD and High Energy Interactions, 32nd Rencontres de Moriond, Les Arcs, France, March 22-29, 1997.
5. K. Goulianos, *Factorization and scaling in hard diffraction*, Proceedings of the 5th International Workshop on Deep Inelastic Scattering and QCD (DIS-97), Chicago, USA, 14-18 April 1997, pp. 527-532 (AIP Conference Proceedings 407, J. Repond and D. Krakauer, Eds.); hep-ph/9708217 01 Aug 1997.
6. K. Goulianos, *Results on Diffraction*, to appear in Proceedings of the XVIIth International Conference on Physics in Collision, Bristol, UK, 25-27 June 1997; hep-ex/9708004 01 Aug 1997.
7. ZEUS Collaboration: M. Derrick *et al.*, *Measurement of the diffractive structure function in deep inelastic scattering at HERA*, Z. Phys. **C68** (1995) 569; M. Derrick *et al.*, *Diffractive hard photoproduction at HERA and evidence for the gluon content of the pomeron*, Phys. Lett. **B 356** (1995) 129.
8. H1 Collaboration: T. Ahmed *et al.*, Phys. Lett. **B 348** (1995) 681; *ib.* *A measurement and QCD analysis of the diffractive structure function $F_2^{D(3)}$* , Contribution to ICHEP'96, Warsaw, Poland, July 1996; *ib.* *Inclusive measurement of diffractive deep-inelastic ep scattering*, hep-ex/9708016 15 Aug 1997.
9. F. Abe *et al.*, CDF Collaboration, *The Collider Detector at Fermilab*, Nucl. Instrum. Meth. **A 271** (1988) 387; Amidei *et al.*, *ib.* **A 350** (1994) 73.
10. P. Schlein, *Evidence for Partonic Behavior of the Pomeron*, Proceedings of the International Europhysics Conference on High Energy Physics, Marseille, France, 22-28 July 1993 (Editions Frontieres, Eds. J. Carr and M. Perrottet).
11. K. Goulianos, *Renormalization of hadronic diffraction and the structure of the pomeron*. Phys. Lett. **B 358** (1995) 379; Erratum **B363** (1995) 268.
12. F. Abe *et al.*, CDF Collaboration, *Observation of rapidity gaps in $\bar{p}p$ collisions at 1.8 TeV*, Phys. Rev. Lett. **74**, 855 (1995).
13. S. Abachi *et al.*, DØ Collaboration, *Jet production via strongly-interacting color-singlet exchange in $p\bar{p}$ collisions*, Phys. Rev. Lett. **76**, 734 (1996).
14. M. Derrick *et al.*, ZEUS Collaboration. *Rapidity gaps between jets in photoproduction at HERA*, Phys. Lett. **B369**, 55 (1996).
15. F. Abe *et al.*, CDF Collaboration, *Measurement of $\bar{p}p$ single diffraction dissociation at $\sqrt{s} = 546$ and 1800 GeV*, Phys. Rev. **D50** (1994) 5535.
16. J. Whitmore, *Diffractive parton distribution functions and factorization tests*, Proceedings of the 5th International Workshop on Deep Inelastic Scattering and QCD (DIS-97), Chicago, USA, 14-18 April 1997, pp. 564-569 (AIP Conference Proceedings 407, J. Repond and D. Krakauer, Eds.).
17. K. Goulianos and J. Montanha, *Factorization and scaling in soft diffraction*, paper in preparation.